

This article appeared in a journal published by Elsevier. The attached copy is furnished to the author for internal non-commercial research and education use, including for instruction at the authors institution and sharing with colleagues.

Other uses, including reproduction and distribution, or selling or licensing copies, or posting to personal, institutional or third party websites are prohibited.

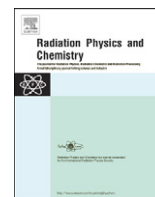
In most cases authors are permitted to post their version of the article (e.g. in Word or Tex form) to their personal website or institutional repository. Authors requiring further information regarding Elsevier's archiving and manuscript policies are encouraged to visit:

<http://www.elsevier.com/copyright>



Contents lists available at ScienceDirect

Radiation Physics and Chemistry

journal homepage: www.elsevier.com/locate/radphyschemValence band study of $\text{LaNiO}_{3-\delta}$ thin filmsS. Grebinskij^a, M. Senulis^a, H. Tvardauskas^a, V. Bondarenka^a, V. Lisauskas^a, K. Sliuziene^a, B. Vengalis^a, B.A. Orlowski^b, R.L. Johnson^c, S. Mickevičius^{a,*}^a Institute of Semiconductor Physics, Center for Physical Sciences and Technology, A. Gostauto 11, LT-01108 Vilnius, Lithuania^b Institute of Physics, Polish Academy of Sciences, Al. Lotnikow 32/46, 02-668 Warsaw, Poland^c Hamburger Synchrotronstrahlungslabor HASYLAB am Deutschen Elektronen-Synchrotron DESY, Notkestr. 85, D-22603 Hamburg, Germany

ARTICLE INFO

Article history:

Received 14 July 2010

Accepted 3 February 2011

Available online 18 February 2011

Keywords:

Rare-earth alloys and compounds

Resonance photoemission

Valence band electronic structure

Oxide materials

ABSTRACT

The resonant photoemission spectroscopy was used to study the surface electronic structure under $\text{La } 4d \rightarrow 4f$ and $\text{Ni } 3p \rightarrow 3d$ photo-excitation of thin $\text{LaNiO}_{3-\delta}$ films after annealing in ultrahigh vacuum above dehydration temperature.

The giant resonance in $\text{La } 5p$ and $\text{La } 5s$ peaks intensity observed at excitation energy corresponding to a $\text{La } 4d \rightarrow 4f$ threshold is accompanied by resonance of the $\text{N}_{4,5}\text{O}_{2,3}\text{O}_{2,3}$ and $\text{N}_{4,5}\text{O}_{2,3}\text{V}$ Auger peaks. The enhancement in the intensity of valence band maxima (at about 6 eV) may be explained by the small mixing of the $\text{La } 5d$ ionic character to the $\text{O } 2p$ valence band. The weak resonant features observed in the valence band spectra under $\text{Ni } 3p \rightarrow 3d$ threshold indicate the loss of nickel species at the $\text{LaNiO}_{3-\delta}$ film surface after heat treatment.

© 2011 Elsevier Ltd. All rights reserved.

1. Introduction

LaNiO_3 is one of the few conductive oxides with a crystal structure suitable for integration in epitaxial heterostructures with perovskites of enormous technological potential such as colossal magnetoresistance materials, high-temperature superconductors and ferroelectrics. It is known that the considerable surface segregation of elements may take place in LaNiO_{3-x} samples and is the tendency of rare-earth and nickel oxides to absorb water vapor and carbon dioxide from air, so that any *ex situ* exposure of these films to air will result in an uncontrolled reaction and surface stoichiometry variation (Choisnet et al., 1994; Li et al., 2004). Thus the knowledge of the surface composition is extremely important because it is directly related to the heterostructure properties.

In the previous paper (Mickevičius et al., 2006) by means of X-ray photoelectron spectroscopy (XPS) using $\text{Mg } K_{\alpha}$ excitation ($h\nu=1253.6$ eV), it was shown that even the short time (about 2 h) exposure to air leads to the formation of the hydroxide layer on the film surface. The escape depth at this photon excitation energy is about 4 monolayers (ML) (Briggs and Seach, 1996) for the $\text{La } 3d$ and $\text{Ni } 2p$ spectra of interest.

Angle dependent spectra, obtained with synchrotron X-rays at much higher energies ($h\nu=3000$ eV, escape depth about 10 ML), revealed that significant variations in oxide vs. hydroxide

concentrations occurred within the relatively thin surface layer even after long-term (one year) exposure to the atmosphere. Estimated thickness of this hydroxide enriched layer was 6 ± 1 ML (Mickevičius et al., 2007).

The initially hydrated LaNiO_{3-x} surface may be restored by heating above dehydration temperature (Samata et al., 2007; Milt et al., 2003). Nickel hydroxide, in turn, decomposes at $T > 230$ °C (melting point) (Sakashita and Sato, 1973). When heated above decomposition temperature it emits toxic fumes of metallic nickel, and one would expect a decrease in Ni-species relative concentration in the previously hydrated surface layer.

So far there have been many studies on LaNiO_3 electronic structure by means of different photoemission spectroscopy techniques (Barman et al., 1994; Sarma et al., 1995; Horiba et al., 2007; Eguchi et al., 2009). A powerful tool to investigate the electronic properties of d and f metals compound surface is resonant photoemission spectroscopy. In this technique the radiation energy $h\nu$ is tuned to reach the resonant electron transition, e.g. $3p \rightarrow 3d$ for transition metal ($h\nu \sim 30\text{--}90$ eV) or $4d \rightarrow 4f$ for rare-earth atoms ($\sim 100\text{--}200$ eV), in order to excite locally and selectively the electrons in the particular chosen atom. The escape depth of electrons leaving the crystal depends strongly on their kinetic energy and reaches a minimum value of ~ 2 ML at kinetic energy of escaping electron ~ 90 eV (Briggs and Seach, 1996). This is the reason why the resonant photoemission spectra become a powerful tool for studying surface electronic structure.

The aim of our work is to investigate the surface electronic structure and chemical composition of LaNiO_{3-x} thin films after heating above dehydration temperature ~ 500 °C.

* Corresponding author.

E-mail address: sigism@pfi.lt (S. Mickevičius).

2. Experimental

Thin LaNiO_{3-x} films onto monocrystalline (1 0 0)-plane oriented NdGaO_3 substrate were deposited using a reactive DC magnetron sputtering technique. The ceramic LaNiO_3 target (25 mm in diameter and 2.5 mm in thickness) was prepared by pressing at 5×10^8 Pa and after sintering in air at 1000 °C for 10 h the La_2O_3 and NiO (99.99% purity from Aldrich-Chemie) powders in the stoichiometric ratio. The sputtering was performed in Ar and O_2 mixture (20:1) at pressure of about 15 Pa. To prevent the film bombardment by high energy ions during deposition, NdGaO_3 substrates were positioned in “off-axis” configuration at a distance of 15 mm from the symmetry axis of the discharge and 20 mm over the target plane. The substrate temperature was ~ 750 °C. Under these conditions, the deposition rate was 25 nm/h, and the resultant thickness of LaNiO_{3-x} film was about 0.1 μm .

The film was annealed at 560 °C under ultrahigh vacuum (UHV) $\sim 10^{-10}$ Torr conditions for 10 h. Additional Ar^+ ion sputtering at 600 V and current density $0.5 \mu\text{A cm}^{-2}$ for 15 min was used to remove surface contamination. The resonant photoemission experiments were performed in the synchrotron radiation laboratory HASYLAB, Hamburg (Germany). Synchrotron radiation from the storage ring DORIS III was monochromatized using plane grating monochromator (FLIPPER II) for the photon energy range of 15–200 eV. The spectrometer was equipped with a CMA electron energy analyzer. The total energy resolution was kept at 0.1 eV. The origin of the energy axis was set at the Fermi level of Au sample, which was electrically connected to the thin film samples (Shirley (1972)).

After the Shirley background subtraction, the complex photoelectron spectra were decomposed into separate peaks by specifying the peak position, binding energy (BE), area, width and Gaussian/Lorentzian ratio. The accuracy of the measured lines BE and relative intensities were about 0.1 eV and 10%, respectively.

3. Results and discussion

3.1. Normalization procedure

To compare photoelectron spectra obtained at different excitation photon energies one needs an appropriate normalization procedure to adjust measurements. In the absence of data required for normalization to the photon flux, the adventitious contamination peaks such as O 2p signal of surface oxygen (at about 6 eV binding energy) in the case of metallic lanthanum (Sairanen et al., 1991) or contamination peaks from carbon monoxide at around ~ 10 eV for metal oxides may be used for normalization (Park et al., 2004). The photoelectron spectra measured at $h\nu = 58$ eV, i.e. far from both La $4d \rightarrow 4f$ and Ni $3p \rightarrow 3d$ resonance, are presented in Fig. 1 after different treatments. All spectra are normalized to the valence band (VB) maximum. The relatively narrow peak (FWHM $\sim 1.24 \pm 0.08$ eV) at BE ~ 10 eV may be attributed to carbon monoxide contamination (Park et al., 2004). A sequential decrease in this peak intensifies after annealing in UHV at 560 °C for 10 h and Ar^+ ion sputtering indicates that the peak is partly derived from the surface contamination resulting from CO absorption.

The photon energy dependence of adventitious peak intensity includes not only the intensity of the monochromatized photon flux, but also the cross-section and escape depth spectral distribution and may be used as a reference for the spectra normalization. This procedure is reasonable since peak at around ~ 10 eV arises from the binding state 5σ of oxygen 2p and carbon $2s/2p$ orbitals in CO, their photon energy dependence of the cross-section is similar to

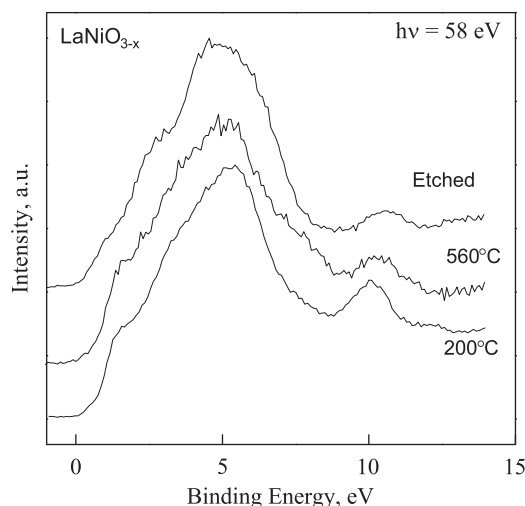


Fig. 1. Photoelectron spectra of LaNiO_{3-x} thin film valence band region measured after annealing in UHV at 200 and 560 °C and subsequent Ar^+ ion sputtering; excitation energy $h\nu = 58$ eV.

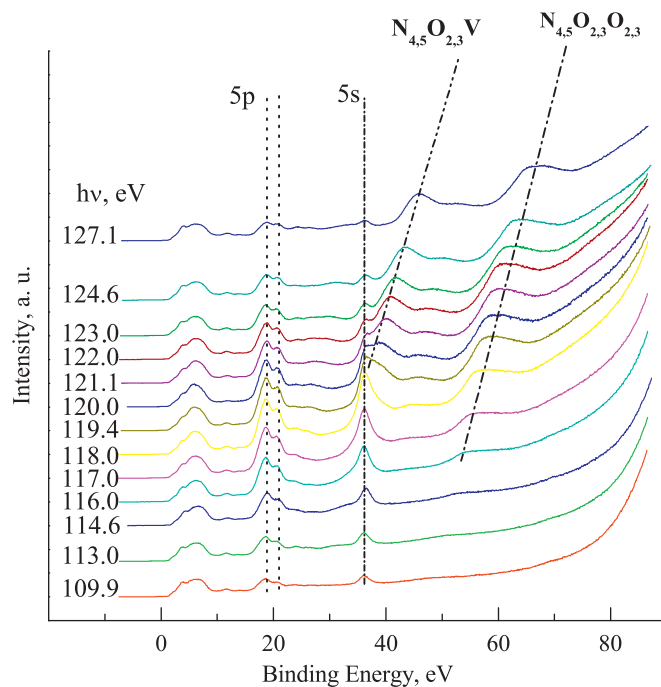


Fig. 2. Set of EDC for the VB, core-level (La 5s and La 5d) and Auger ($\text{N}_{4,5}\text{O}_{2,3}\text{O}_{2,3}$ and $\text{N}_{4,5}\text{O}_{2,3}\text{V}$) electrons in LaNiO_{3-x} thin film recorded around the lanthanum $\text{La}4d \rightarrow 4f$ threshold energy. Excitation energies are also shown.

that of oxygen 2p (Yeh and Lindau, 1984; Wilhelmy et al., 1994; Plummer et al., 1997).

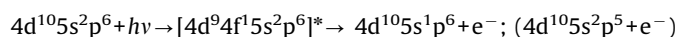
3.2. Core-level spectra

A set of energy distribution curves (EDC) of LaNiO_{3-x} film for the photon energy range covering the energy of the La $4d \rightarrow 4f$ transition is shown in Fig. 2. In the photoelectron spectra there are four different line groups: VB region, La 5s at $\text{BE} = 36.2 \pm 0.3$ eV, La $5p_{3/2}$ at $\text{BE} = 18.3 \pm 0.3$ eV and La $5p_{1/2}$ at $\text{BE} = 20.5 \pm 0.3$ eV. One can see the $\text{N}_{4,5}\text{O}_{2,3}\text{O}_{2,3}$ and $\text{N}_{4,5}\text{O}_{2,3}\text{V}$ Auger peaks at the kinetic energies (KE) of 62.3 ± 0.1 eV and 81.5 ± 0.1 eV, respectively (Riviere et al., 1985; Rihcter et al., 1988). These results are in an agreement with the data reported for $4d \rightarrow 4f$ excitations in metallic lanthanum

(Sairanen et al., 1991). Slight BE shift of 1.2 eV for La 5s and 5p lines towards higher energies may be attributed to the Coulomb interaction in ionic compounds. The Coulomb interaction also leads to a slight energy shift of 0.7 eV towards lower KE in the case of $N_{4.5}O_{2.3}V$ transition, while KE for $N_{4.5}O_{2.3}O_{2.3}$ transition is actually the same as for metallic lanthanum.

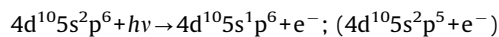
Photon energy dependencies of the relative intensities of the different Auger and photoelectron lines, Constant Initial State (CIS) spectra, observed for $LaNiO_{3-x}$ films in the vicinity of the La 4d → 4f threshold are displayed in Fig. 3. The relative intensities of these four lines have been determined by spectra fitting after the Shirley background removal.

The giant resonance observed for lanthanum 5s; (5p) core levels may be explained by an autoionization process (Sairanen et al., (1991)), leading to the emission of ejected electron after the resonant La 4d → 4f excitation:



where * denotes the excited state.

In this process the energy of emitted electron is the same as it had been produced by direct photoemission of an electron from the 5s; (5p) orbital expressed by



The direct photoemission occurs in a wide range of $h\nu$ energies, while the additionally ejected electrons are excited in the resonant photoemission energy region corresponding to 4d → 4f threshold, and in photoelectron spectra these processes are seen as enhanced intensity of corresponding photopeaks. The contribution of resonance photoemission can be described by the Fano formula introduced for atomic systems and illustrated by the Fano line shape with the resonant maximum followed by the anti-resonant minimum (Fano, 1961; Sonntag and Zimmermann, 1992).

This result is reiterated in CIS spectra (see Fig. 3), where the photon energy is scanned through the resonance, and the exitation spectrum has a specific shape called the Fano profile. The resonant structure also appears in the Auger $N_{4.5}O_{2.3}O_{2.3}$ and $N_{4.5}O_{2.3}V$ transitions (Fig. 3a) in an agreement with an autoionization model of resonance process after 4d → 4f excitation (Aksela et al., 1988; Bancroft et al., 1990). Full lines illustrate that the Fano profiles were calculated using the following formula:

$$I(h\nu) = I_0 \frac{(\varepsilon + q)^2}{1 + \varepsilon^2} \quad (1)$$

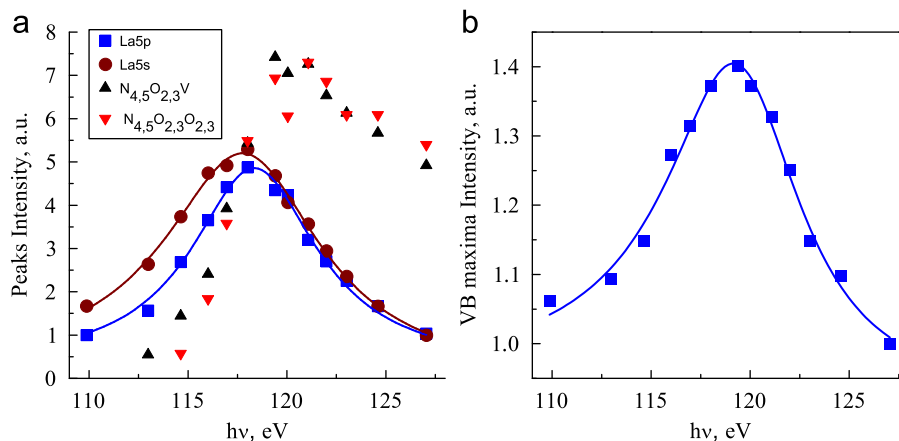


Fig. 3. Photon energy dependencies of the relative photoelectron intensities, CIS spectra of lines corresponding (a) to the Auger ($N_{4.5}O_{2.3}O_{2.3}$ and $N_{4.5}O_{2.3}V$) and photoelectron (5p and 5s) transitions and (b) at valence band intensity maximum for $LaNiO_{3-x}$ films in the vicinity of the La 4d → 4f threshold. Lines corresponds to the fitted Fano profiles.

where $\varepsilon = h(\nu - \nu_{res})/w$, w describes spectral width of the autoionized discrete state, q is Fano's asymmetry parameter and I_0 is the intensity of nonresonant photoemission. We obtained $I_0 = 4.6 \pm 0.2$, $w = 3.9 \pm 0.3$ eV and $q = 4.9 \pm 2.2$ for La 5p peak, and $I_0 = 5.1 \pm 0.18$, $w = 4.8 \pm 0.3$ eV and $q = 4.8 \pm 2.6$ for La 5s peak.

3.3. Valence band spectra

In this section results of detailed study of VB photoelectron spectra in the vicinity of La 4d → 4f and Ni 3p → 3d resonant transitions are presented.

A set of valence band EDCs taken at La 4d → 4f transition energies is shown in Fig. 4. Beyond the giant resonance observed for lanthanum 5s and 5p core levels (see Fig. 2), a relatively weaker resonance structure was also observed for valence band photoemission at the La 4d → 4f threshold. The CIS spectra at valence band intensity maximum for $LaNiO_{3-x}$ films in the vicinity of the La 4d → 4f threshold are shown in Fig. 3b. The full line illustrates that the Fano profile was obtained by formula (1) using $I_0 = 0.47 \pm 0.03$, $w = 4.15 \pm 0.38$ eV and $q = 4.7 \pm 2.9$ values.

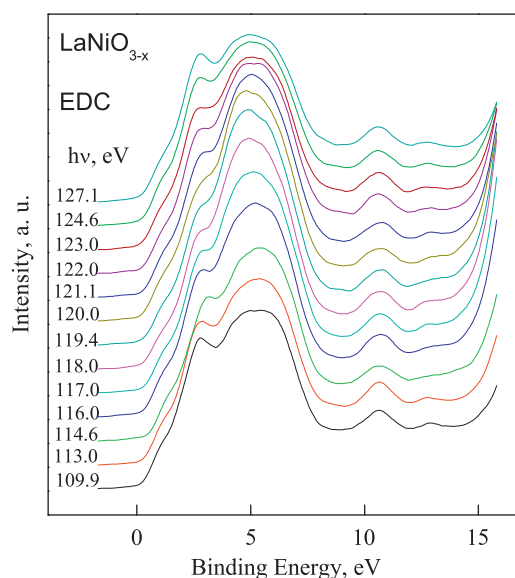


Fig. 4. Set of EDC for the valence-shell electrons in $LaNiO_{3-x}$ thin film recorded around the lanthanum La 4d → 4f threshold energies. Excitation energies are also shown.

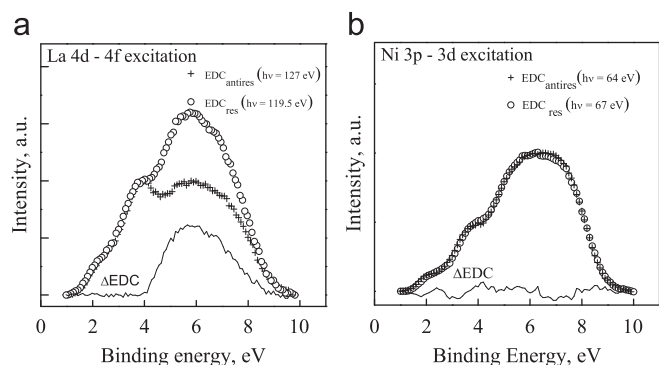


Fig. 5. EDCs showing the valence band of (annealed at 560 °C) thin LaNiO_{3-x} film spectra after the Shirley background removal (a) at the La 4d \rightarrow 4f and (b) at the Ni 3p \rightarrow 3d excitation for resonance and anti-resonance photon energies. The curves below represent the results of the difference in spectrum $\Delta\text{EDC} = \text{EDC}_{\text{res}} - \text{EDC}_{\text{anti-res}}$.

Fig. 5a shows EDC's valence band region of LaNiO_{3-x} film at the La 4d \rightarrow 4f threshold for resonance and anti-resonance photon energies. The resonance observed in the VB intensity maximum may be related to a small admixture of La 5d character to O 2p valence band. In Fig. 5a, the difference between resonance ($h\nu = 119.5$ eV) and anti-resonance ($h\nu = 127$ eV) photoemission spectra clearly indicates that only bonding (i.e. O 2p σ) states at around 5–7 eV (Park et al., 2004; Mullica et al., 1993) participate in the observed VB enhancement, while peak at around 3 eV corresponding to nonbonding O 2p π molecular orbital is actually insensitive to resonant La 4d \rightarrow 4f excitation.

Flavell et al. (1995) reported the resonant photoemission study of $\text{La}_{1-x}\text{Sr}_x\text{Ni}_{1-y}\text{Fe}_y\text{O}_{4+\delta}$ at the Ni 3p \rightarrow 3d threshold. The observed resonance was considerably weaker than for the d \rightarrow f transition, but it is nevertheless seen clearly in the CIS data. The 3p–3d resonant effects are interpreted in a similar way to the d–f resonance described above and are attributed to interference between direct and indirect channels. The direct photoemission occurs in a wide range of excitation energies, while the additionally ejected electrons are excited in the resonant photoemission energy region corresponding to the 3p \rightarrow 3d transition energy region.

Fig. 5b shows EDC's valence band region of LaNiO_{3-x} film at the Ni 3p \rightarrow 3d threshold for resonance and anti-resonance photon energies. In resonant photoemission spectroscopy the differences in EDC measured for resonant and anti-resonant energy show the contribution of transition metal 3d electrons to the valence band density of states. As shown in Fig. 5b, the observed resonance was weak similarly as in $\text{La}_{1-x}\text{Sr}_x\text{Ni}_{1-y}\text{Fe}_y\text{O}_{4+\delta}$ at the Ni 3p \rightarrow 3d threshold (Flavell et al., 1995). One of the reason of these results can be the small amount of nickel species at the film surface. The electron escape depth depends strongly on the kinetic energy of the emitted electrons. In the case of this experiment the escape depth is about 2 ML. The LaNiO_{3-x} film after exposure to air the hydroxide enriched layer ~ 6 ML is formed at the surface, which after heating above dehydration temperature 550 °C can lose the Ni-species. This result requires the further studies on chemical composition, surface morphology and electronic structure of hydrated LaNiO_{3-x} surface layer.

4. Summary and conclusions

We have examined the surface electronic structure of LaNiO_{3-x} thin films after heating above dehydration temperature by means of resonant photoemission spectroscopy using tunable synchrotron radiation.

The giant resonance in La 5p and La 5s peaks intensity observed at excitation energy corresponding to a La 4d \rightarrow 4f threshold is accompanied by resonance of the $\text{N}_{4,5}\text{O}_{2,3}\text{O}_{2,3}$ and $\text{N}_{4,5}\text{O}_{2,3}\text{V}$ Auger peaks. The obtained results are in an agreement with the model of an autoionization process after resonant excitation.

The enhancement in the intensity of valence band maxima (at about 6 eV) may be explained by the small mixing of the La 5d ionic character to the O 2p valence band.

The weak resonant features were observed in the VB spectra under Ni 3p \rightarrow 3d excitation (escape depth $L \approx 2$ ML), indicating that losses of nickel species take place at the LaNiO_{3-x} film surface after heat treatment in ultrahigh vacuum.

Acknowledgment

This work was partially supported by DESY and the European Commission under Contract RII3-CT-2004-506008 (IA-SFS) project DESY-D-I-20070119 EC.

References

- Aksela, S., Sairanen, O.-P., Aksela, H., Bancroft, G.M., Tan, K.H., 1988. Normal and resonance LVV Auger spectra of gas-phase SiC_4 molecules. *Phys. Rev. A* 37, 2934–2940.
- Bancroft, G.M., Tan, K.H., Sairanen, O.-P., Aksela, S., Aksela, H., 1990. Decay processes after resonant excitation of S 2p and F 1s electrons in SF_6 molecules. *Phys. Rev. A* 41, 3716–3722.
- Barman, S.R., Chainani, A., Sarma, D.D., 1994. Covalency-driven unusual metal-insulator transition in nickelates. *Phys. Rev. B* 49, 8475–8478.
- Briggs, D., Seach, M.P., 1996. *Practical Surface Analysis by Auger and X-ray Photoelectron Spectroscopy*. John Wiley & Sons Ltd., Chichester–New York, p. 674.
- Choisnet, J., Abadzhieva, P., Stefanov, N., Klissurski, D., Bassat, J.M., Rives, V., Minchev, L., 1994. X-ray photoelectron spectroscopy, temperature-programmed desorption and temperature-programmed reduction study of LaNiO_3 and $\text{La}_2\text{NiO}_{4+\delta}$ catalysts for methanol oxidation. *J. Chem. Soc. Faraday Trans. 90*, 1987–1991.
- Eguchi, K., Chainani, A., Taguchi, M., Matsunami, M., Ishida, Y., Horiba, K., Senba, Y., Ohashi, H., Shin, S., 2009. Fermi surfaces, electron-hole asymmetry, and correlation kink in a three-dimensional Fermi liquid LaNiO_3 . *Phys. Rev. B* 79, 115122–115122-6.
- Fano, U., 1961. Effects of configuration interaction on intensities and phase shifts. *Phys. Rev.* 124, 1866–1878.
- Flavell, W.R., Hollingworth, J., Howlett, F., Thomas, A.G., Sarker, Md.M., Squire, S., Hashim, Z., Mian, M., Wincott, P.L., Teehan, D., Downes, S., Hancock, F.E., 1995. Resonant photoemission from complex cuprates and nickelates. *J. Synchrotron Radiat.* 2, 264–271.
- Horiba, K., Eguchi, R., Taguchi, M., Chainani, A., Kikkawa, A., Senba, Y., Ohashi, H., Shin, S., 2007. Electronic structure of LaNiO_{3-x} : an in situ soft X-ray photoemission and absorption study. *Phys. Rev. B* 76, 155104–1–155104-6.
- Li, Y., Chen, N., Zhou, J., Song, S., Liu, L., Yin, Z., Cai, C., 2004. Effect of the oxygen concentration on the properties of Gd_2O_3 thin films. *J. Cryst. Growth* 265, 548–552.
- Mickevičius, S., Grebinkij, S., Bondarenka, V., Vengalis, B., Šliužienė, K., Orlowski, B.A., Osinniy, V., Drube, W., 2006. Investigation of epitaxial LaNiO_{3-x} thin films by high-energy XPS. *J. Alloys Compd.* 423 (2006), 107–111.
- Mickevičius, S., Grebinkij, S., Bondarenka, V., Lisauskas, V., Šliužienė, K., Tvardauskas, H., Vengalis, B., Orlowski, B.A., Osinniy, V., Drube, W., 2007. The surface hydro-oxidation of $\text{LaNiO}_{3-\delta}$ thin films. *Acta Phys. Polon. A* 112, 113–120.
- Milt, V.G., Querini, C.A., Miro, E.E., 2003. Thermal analysis of $\text{K}(x)/\text{La}_2\text{O}_3$, active catalysts for the abatement of diesel exhaust contaminants. *Thermochim. Acta* 404, 177–186.
- Mullica, D.F., Perkins, H.O., Lok, C.K.C., Young, V., 1993. The X-ray photoemission of $\text{La}(\text{OH})_3$. *J. Electron Spectrosc. Relat. Phenom.* 61, 337–355.
- Park, J., Oh, S.-J., Park, J.-H., Kim, D.M., Eom, C.-B., 2004. Electronic structure of epitaxial $(\text{Sr,Ca})\text{RuO}_3$ films studied by photoemission and X-ray absorption spectroscopy. *Phys. Rev. B* 69, 085108–1–085108-6.
- Plummer, E.W., Gustafsson, T., Gudart, W., Eastman, D.E., 1997. Partial photoionization cross sections of N_2 and CO using synchrotron radiation. *Phys. Rev. A* 15, 2339–2355.
- Rihcter, M., Th., Prescher, Meyer, M., von Raven, E., Sonntag, B., Askela, S., 1988. Solid-state binding, recombination and Auger energy shifts of rare-earth metals. *Phys. Rev. B* 38, 1763–1772.
- Riviere, J.C., Netzer, F.P., Rosina, G., Strasser, G., Matthew, J.A., 1985. The 4d Auger, Coster-Kronig and recombination spectra of the lanthanides. *J. Electron Spectrosc. Relat. Phenom.* 36, 331–375.

- Sairanen, O.-P., Askela, S., Kivimäki, A., 1991. Resonance Auger and autoionization process in solid lanthanum after 4d→4f resonant excitation by synchrotron radiation. *J. Phys.: Condens. Matter* 3, 8707–8716.
- Sakashita, M., Sato, N., 1973. The structure and reactivity of nickel hydroxide. *Bull. Chem. Soc. Jpn.* 46, 1983–1987.
- Samata, H., Kimura, D., Saeki, Y., Nagata, Y., Ozawa, T.C., 2007. Synthesis of lanthanum oxyhydroxide single crystals using an electrochemical method. *J. Cryst. Growth* 304, 448–451.
- Sarma, D.D., Shanthi, N., Barman, S.R., Hamada, N., Sawada, H., Terakura, K., 1995. Band theory for ground-state properties and excitation spectra of perovskite LaMO_3 (M=Mn, Fe, Co, Ni). *Phys. Rev. Lett.* 75, 1126–1129.
- Shirley, D.A., 1972. High-resolution X-Ray photoemission spectrum of the valence bands of gold. *Phys. Rev. B* 5, 4709–4714.
- Sonntag, B., Zimmermann, P., 1992. XUV spectroscopy of metal atoms. *Rep. Prog. Phys.* 55, 911.
- Wilhelmy, I., Lutz, A., Görling, A., Rösch, N., 1994. Molecular photoionization cross sections by the Lobatto technique. I. Valence photoionization. *J. Chem. Phys.* 100, 2808–2820.
- Yeh, J.J., Lindau, I., 1984. Atomic subshell photoionization cross sections and asymmetry parameters: $1 \leq Z \leq 103$. *At. Data Nucl. Data Tables* 32, 1–155.